Wear 406–407 (2018) 166–172

Contents lists available at ScienceDirect

Wear

journal homepage: www.elsevier.com/locate/wear

Anti-erosive mechanism of a grooved surface against impact of particle-laden flow

Sohyun Jung, Eunjin Yang, Wonjong Jung, Ho-Young Kim*

Department of Mechanical and Aerospace Engineering, Seoul National University, Seoul 08826, Republic of Korea

ARTICLE INFO

Keywords:
Impact wear
Solid particle erosion
Erosion testing
Surface topography
Bio-tribology

ABSTRACT

Erosion is a mechanical process that determines the lifetime of many machine components, as well as the quality of the protective skins of some animals and plants. Here, we assess quantitatively the role of grooves on ductile erosive surfaces in reducing erosion caused by the impact of particle-laden flow. In particular, we focus on V-shape grooves that are much larger than the particles. The grooves can induce diversification of impingement angles, multiple impacts of a single particle, and air swirls. By measuring the erosion rates of smooth and grooved surfaces at different impingement angles, and imaging the particle motion with a high-speed camera, we show that the diversified impingement angle on the grooves plays a key role in reducing erosion. Further, we predict theoretically the optimal groove angle for maximal erosion reduction at different values of impact angle. Our findings provide a framework for the design of artificial anti-erosive surfaces and advance our understanding of the design principles that enable biological skins to display anti-erosive properties when subjected to particle-laden fluid streams.

1. Introduction

The lifetimes of many machinery components and construction materials are influenced significantly by their capacity to resist erosion and corrosion. Corrosion, a chemical/electrochemical reaction that destroys the material, is enhanced by the erosion of the material surface [1]. Therefore, understanding and controlling erosion play important roles in many industries [2–4]. Furthermore, erosion is responsible for shaping the earth through processes such as rainfall, river streams, sea waves, glacial motions, and landslides [5]. Among many physical causes contributing to the erosion of industrial and natural objects, here we are interested in the erosion caused by the impact of fluid flows laden with solid particles, e.g., slurry flows and dusty winds. Industrial examples that suffer from erosion mediated by the impact of particle-laden flows include slurry and powder transfer pipelines, the blades of wind power generators and turbomachinery, and outer panels of vehicles.

Previous research has shown that the impact of particles can cut, plastically deform, or fracture material's surface [6]. The factors affecting the rate of impact-induced erosion have been identified as the impingement angles [7–12], the impact velocity of the solid particles [9–15], the substrate properties [9,10,16], total mass of impacted particles [9,11,12,16], particle size [10,11,17–19], and particle shape [12,19,20]. A number of technologies have been developed to reduce such erosion, including a filter system [21,22], anti-erosion materials [23,24], and surface treatments such as chemical coating [25–27], laser treatment [28–30], and patterning [31–34].

Recently, there has been a growing interest in the anti-erosion mechanism of living creatures inhabiting harsh environments. Several creatures that live in the desert, e.g., a snake [35], sand fish [36], and scorpion [37], possess certain textures on their surface, which are known to effectively resist abrasive erosion. In addition, tamarisk trees that are found in dry environments with frequent sandstorms, are known to have corrugated barks that are resistant to erosion caused by the impact of sand particles [38]. Although the biologically-inspired surface texturing to reduce erosion is highly attractive for practical applications, the fundamental mechanism that underlies such anti-erosive performance currently remain elusive.

Numerical computations of flow fields around various groove patterns and consequent flow-induced erosion rates suggested that swirling airflow inside the grooves acts as an air cushion to weaken the impact of solid particles [31,32]. However, the proposed mechanism has not been supported by experimental measurements to date. In addition, other plausible functions of grooves such as their capacity to change particle impingement angle and the effect of multiple particle impacts upon reflection have not been investigated. Therefore, in the present work, we measured experimentally the erosion rates of smooth and grooved surfaces to quantify the anti-erosive characteristics of the

* Corresponding author.
E-mail address: hyk@snu.ac.kr (H.-Y. Kim).

https://doi.org/10.1016/j.wear.2018.04.008
Received 11 September 2017; Received in revised form 11 April 2018; Accepted 11 April 2018
Available online 13 April 2018
0043-1648/

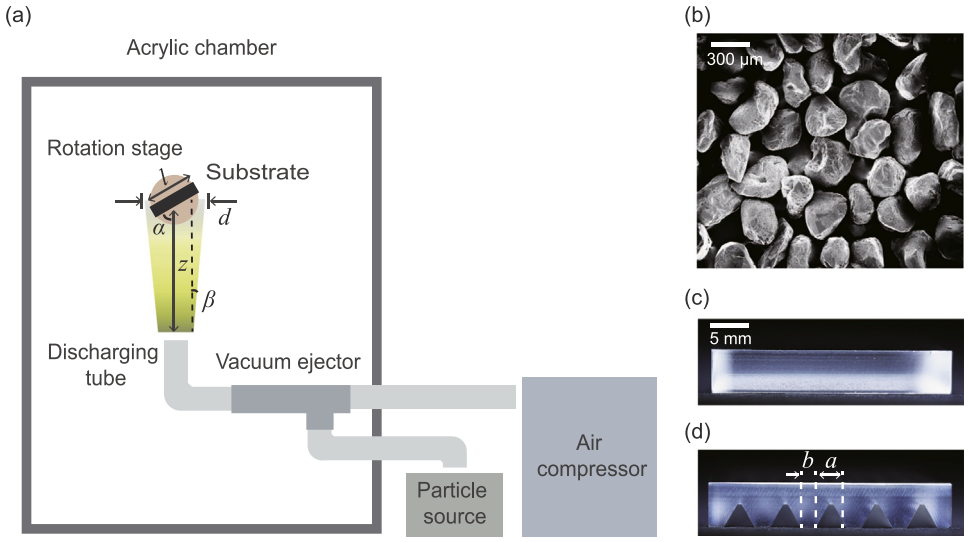

Fig. 1. (a) A schematic diagram of the experimental apparatus used to measure the erosion rates caused by particle-laden flow. The distance from the discharge tube and the center of the substrate is denoted as z, and d is the actual diameter of the particle stream. The side length of the square substrate is marked as l. α and β represent the impingement angle and the finite degree of particle dispersion, respectively. (b) SEM (scanning electron microscopy) image of quartz sand particles. (c) Side view of the smooth substrate. (d) Side view of the grooved surface with five equilateral triangular trenches.

patterned surfaces. The results of the measurements allowed us to identify the dominant mechanism of anti-erosive activity of the grooved surfaces over a finite range of impingement angles.

2. Materials and methods

The experimental apparatus used to generate particle-laden flows and to measure the erosion rates of substrates is schematically shown in Fig. 1(a). In a transparent acrylic chamber, a tube ejects high-speed airflow carrying particles onto a substrate at an impingement angle α, controlled by a rotation stage from 10° to 90°. The particle discharging tube is connected to a vacuum ejector that draws particles and air from a particle container and an air compressor, respectively. For the particles, we used white quartz sand (Sigma Aldrich), as shown in Fig. 1(b), whose average diameter and density are 230 μm and 2530 kg m^{-3}, respectively. The average diameter of the particles is defined as the diameter of a circle that has the same average area as the cross-sectional image of the grains. During the experiments, compressed air was injected into the vacuum ejector at a flow rate of 60 L min^{-1}, which drew the particles at a rate of 2.83 g s^{-1} and mixed them with the air. The particles were expelled through the discharging tube (6.5 mm inner diameter) at an exit velocity of 19 m s^{-1} as measured by a high-speed camera (Photron SA 1.1). The superficial velocity of air, U, was U = 30 m s^{-1} as measured by an air velocity meter (TSI VelociCalc 8346). We note that the wind speed in nature is typically below 20 m s^{-1} [39], which corresponds to a typical driving speed of automobiles.

As the substrate, we used an acrylic plate with a tensile strength and Young's modulus of 71.3 MPa and 3.2 GPa, respectively. We used two different types of surface morphology—smooth surfaces and V-shape grooved surfaces reported to be more anti-erosive than many of differently shaped grooves including U-, square-, and dome-shapes. [32]. For the smooth surface, we used a pristine surface with a roughness (defined as the ratio of the actual area to the projected area) of 1.0095 (± 0.0052) as measured by atomic force microscopy (Park Systems XE-70). The grooved surface possesses equilateral triangular trenches as carved by a tapping center. The apex of each triangle is rather blunt because of the limitation in the machining process. We ignored the effect of this bluntness on the results of our analysis since it represents only a very small portion of the entire groove size, and represents a spot where particle impacts is infrequent as a result of the shadowing by adjacent grooves. The triangles have a side of a = 4 mm long, and are spaced by b = 2 mm. The cross-sectional images of the substrates are shown in Fig. 1(c) and (d). The side length of the square substrate l = 32 mm. The distance from the discharge tube to the center of the substrate (z in Fig. 1(a)) is 14 cm.

Each erosion test lasted for one hour, after which we measured the mass loss W of a substrate by comparing its mass to that determined before the run. We repeated each test under the same conditions three times and calculated the average values. In addition, to visualize the particle paths near the substrates and to measure the coefficient of restitution upon impact, we used the high-speed camera running at 3×10^4 frames per second.

3. Results of erosion test

The results of the erosion tests are presented as a function of the impingement angle for both the smooth and the grooved surfaces. The erosion rate is defined as $\Pi = W/M$, which measures the mass loss of a substrate, W, due to the total mass of the impact particle, M. We note that the amount of particles encountering the substrate varies for different substrate orientations. For instance, only fractions of particles emitted from the tube impact onto the substrate with a low impingement angle α. Thus, M is calculated as $M = (L/d)M'$, from the known quantity, M', which represents the total mass of the ejected particles. Here, the projected length of the substrate $L = l \sin\alpha$, and the diameter of the particle stream near the substrate $d \approx 34$ mm, as illustrated in Fig. 1(a).

Fig. 2 shows the experimentally measured erosion rates of both smooth and grooved surfaces at different impingement angles. For the smooth surface, the erosion rate increased for small α until it reached a maximum at α = 20°, and then monotonically decreased. The maximum erosion rate at α = 20° is 3.4 times higher than the minimum value determined at α = 90°. For the grooved surface, the change in the erosion rate with α was relatively mild, and the rate reached its maximum at 10° and minimum at 40°, with the maximum rate being 1.5 times higher than the minimum value. In the following, we first explain the high sensitivity of the smooth surface to α. We then rationalize the erosion rates measured for the grooved surface using the quantitative erosion data for the smooth surface, in order to elucidate the dominant anti-erosive mechanism of the grooves. Finally, we describe a theoretical model to predict the optimal groove angles depending on the impact direction, and provide a rationale for the grooved surface of